A P39R mutation at the N-terminal domain of human αB-crystallin regulates its oligomeric state and chaperone-like activity

Nobutaka Numoto[a], Akiko Kita[a,*], Noriko Fujii[a], Kunio Miki[b]

[a]Research Reactor Institute, Kyoto University, Kumatori, Osaka 590-0494, Japan

[b]Department of Chemistry, Graduate School of Science, Kyoto University, Sakyo-ku, Kyoto 606-8502, Japan

*Corresponding author. Address: Research Reactor Institute, Kyoto University, Kumatori, Osaka 590-0494, Japan

Tel: +81-724-51-2379. Fax: +81-724-51-2635

E-mail address: kita@rri.kyoto-u.ac.jp

Abstract

Recent structure analyses of αB-crystallin have proposed some models of the N-terminal domain and the manner of oligomerization, whereas the effects of the significantly high content of Pro residues at the N-terminal domain remain unclear. We report the properties of a novel P39R mutant of αB-crystallin. The content of α-helix was increased, and the molecular size of the P39R mutant was larger than that of wild-type αB-crystallin. A slight loss of chaperone-like activity was observed using alcohol dehydrogenase (ADH), while a significant increase was detected by insulin assay. The Pro residue at the N-terminal domain of αB-crystallin is important for oligomerization and function.

Keywords:

small heat shock protein, molecular chaperone, quaternary assembly, protein aggregation, secondary structure, cataract

Abbreviations:

ADH, alcohol dehydrogenase; sHSP, small heat shock protein, CD, circular dichroism; SAXS, small-angle X-ray scattering; DLS, dynamic light scattering

Highlights:

The P39R mutant αB-crystallin showed increased α-helix content.

The molecular size of P39R mutant is larger than that of wild-type αB-crystallin.

The P39R mutant displayed a slight loss of chaperone-like activity with ADH assay.

The P39R mutant displayed an increase of the activity with denatured insulin.

The N-terminal Pro plays a key role in oligomerization and function.

Introduction

The transparency of eye lens cells is maintained by a highly abundant protein known as α-crystallin, which is composed of αA- and αB-crystallins [1]. Both proteins belong to the small heat shock protein (sHSP) family and function as molecular chaperones to prevent the aggregation of other proteins when exposed to certain types of stress [2]. Structural anomalies such as point mutations of α-crystallin genes [3] or racemization and isomerization of certain residues by UV irradiation [4,5] are known to cause human cataracts. The expression of αB-crystallin is widespread in many tissues, including muscle and brain, and has been implicated in myopathies [6], Alexander disease [7], and Alzheimer's disease [8]. For decades, researchers have attempted to describe the high-resolution structure of αB-crystallin, which is composed of a core structure conserved among all sHSPs that is referred to as the α-crystallin domain and highly flexible N- and C-terminal domains [9]. The crystal structures of truncated forms containing the α-crystallin domain and a portion of the C-terminal domain [10,11], together with solid-state NMR measurements of full-length αB-crystallin [12], have demonstrated that a stable homodimer is formed by the β-sheets of the α-crystallin domain. However, the flexible N- and C-terminal domains yield diverse oligomerization states [13] and prevent the crystallization needed for high-resolution structure determination. Recent studies of a quaternary assembly of αB-crystallin based on EM, solid-state NMR, and small-angle X-ray scattering (SAXS) analyses proposed homo-oligomer models of 24-meric assembly [14,15,16]. The models also provide reasonable explanations for the heterogeneity of αB-crystallin via the dynamic exchange of the dimer subassemblies to form larger oligomerizations such as 26 and 28-mer, and up to 36-mer proteins. On the other hand, these models differ

significantly in terms of how contact is achieved between the N- and C-terminal domains and the neighboring subunit. Therefore, further structure analyses will be needed to elucidate the detailed oligomerization mechanism of αB-crystallin.

Several crystal structures of intact or artificially truncated proteins belonging to the sHSP family have been reported thus far. Wheat HSP16.9 [17] and HSP16.5 from *Methanococcus jannaschii* (MjHSP16.5) [18] consist of 151 and 147 amino acids forming 12 and 24-meric homo-oligomers, respectively. These sHSPs are thought to be highly homologous to 24-meric αB-crystallin composed of 175 amino acids in the monomeric structure. Only in the crystal structure of wheat HSP16.9, almost the entire N- and C-terminal domain regions of the monomer have been identified. The N-terminal domain of wheat HSP16.9 exhibits an α-helix-rich structure, which is in good agreement with the proposed model of the N-terminal domain of αB-crystallin [16]. The amino acid sequence alignment of αB-crystallin with wheat HSP16.9 and MjHSP16.5 (Figure 1) revealed that the N-terminal domain of αB-crystallin contains significantly more Pro residues than do sHSPs. The role played by the high Pro residue content at the N-terminal domain remains poorly understood. However, the conformational rigidity of Pro residues would prevent the formation of stable secondary structures, and thereby could possible account for the flexible properties at the N-terminal domain. It is noteworthy that the position of the Pro39 of αB-crystallin is conserved in MjHSP16.5 (Pro22), but replaced by Arg25 in wheat HSP16.9. Pro22 of MjHSP16.5 was not identified in the crystal structure due to disorder in the N-terminal domain, whereas residues 20-30 of wheat HSP16.9 form a continuous α-helix, which can be clearly observed in the crystal structure. Thus, it would be reasonable to presume that Pro39 plays a key role in defining the structural stability of

the N-terminal domain, which could be expected to affect the oligomeric state and the functions of αB-crystallin.

In this study, we investigated the properties of the oligomeric state and chaperone-like activity of the P39R mutant of αB-crystallin, a novel mutant designed based on protein structure information. Comparisons with the properties of wild-type αB-crystallin revealed that the N-terminal domain is involved in multiple interactions that enable the formation of various oligomers and binding to denatured proteins, thereby enabling chaperone-like activities.

Materials and methods

Expression and purification of recombinant wild-type and P39R mutant αB-crystallins

Escherichia coli BL21(DE3)pLysS was transformed with the vector pET-23d containing human wild-type αB-crystallin cDNA (kind gift of Prof. L. Takemoto). The cells were grown at 37ºC, and expression was induced by 0.3 mM IPTG. Then, the cell cultures were shaken further at 25ºC for 20 h. The cells were harvested and resuspended in 20 mM Tris-HCl pH 8.0 (buffer A) and were disrupted by sonication. The soluble fraction was precipitated by 20% ammonium sulfate on ice, and the supernatant was precipitated by 50% ammonium sulfate. The pellet containing wild-type αB-crystallin was resuspended and dialyzed with buffer A. The cleared lysate was applied to a TOYOPEARL SuperQ-650S column (TOSOH) equilibrated with buffer A and eluted with a linear gradient of 0-0.5 M NaCl. Wild-type αB-crystallin was eluted primarily in the flow-through fraction. The fraction containing wild-type αB-crystallin was concentrated and loaded to a HiLoad 16/60 Superdex 200 column (GE healthcare) equilibrated with buffer A containing 150 mM NaCl and was eluted with the same buffer. The purified protein was desalted and concentrated to 25 mg/ml with buffer A for further experiments.

The P39R mutation was introduced in the wild-type αB-crystallin cDNA using a KOD -Plus- Mutagenesis Kit (TOYOBO) and the mutagenic primer (5’-GAGTCTGATCTTTTCCGGACGTCTACTTCCCTG-3’ and 5’-CAGGGAAGTAGACGTCCGGAAAAGATCAGACTC-3’). The expression plasmids were transformed into *E. coli* Rosetta 2(DE3)pLysS and the cells were grown at 37ºC. Expression was induced by 0.3 mM IPTG, and then the cell cultures were

shaken further at 25ºC for 20 h. The cells were harvested, resuspended in buffer A, and disrupted by sonication. The soluble fraction was applied to a TOYOPEARL SuperQ-650S column (TOSOH) equilibrated with buffer A and eluted with a linear gradient of 0-0.5 M NaCl. The P39R mutant αB-crystallin was eluted primarily in the flow-through fraction. Further purification steps on the gel filtration column were the same as those used for wild-type αB-crystallin.

Circular dichroism (CD) spectroscopy

The far-UV CD spectra of the proteins were recorded by a J-805 spectropolarimeter (JASCO) at 25ºC. The protein concentration was 0.1 mg/ml in 0.1 mM buffer A. A quartz cell with a path length of 1 mm was used, and the reported spectra are the average of five accumulations. The secondary structure contents of the proteins were analyzed using the program JWSSE-480.

Size-exclusion chromatography

The molecular size of the wild-type and the P39R mutant αB-crystallins was determined by size-exclusion chromatography on a 10 × 300 mm Sephacryl S-400 (GE healthcare) column, calibrated by the standard samples (GE healthcare) of thyroglobulin (669 kDa), ferritin (440 kDa), conalbumin (75 kDa), and ribonuclease A (13.7 kDa). The column was equilibrated with 50 mM Tris-HCl pH 8.0 containing 150 mM NaCl. The molecular size of the complexes of denatured proteins and αB-crystallins was determined by the same method.

Dynamic light scattering

Dynamic light scattering (DLS) measurements were carried out using a DynaPro 99 instrument (Protein Solutions). The samples were centrifuged to remove large aggregates and were then loaded onto a 12-μl sample cell (path length, 1.5 mm).

Data were analyzed using the program DYNAMICS version 5.26.56.

Chaperone-like activity assays

The chaperone-like activity of the wild-type and P39R mutant αB-crystallins was assessed by measuring the ability of these proteins to suppress the aggregation of denatured alcohol dehydrogenase (ADH) or insulin, essentially according to the previously reported methods [19,20]. ADH (0.8 mg/ml) was denatured in 50 mM Tris-HCl pH 8.0, 50 mM NaCl, and 10 mM EDTA at 37ºC, in the absence and presence of 0.8 mg/ml or 0.16 mg/ml of αB-crystallins. Insulin (0.33 mg/ml) was denatured in 50 mM Tris-HCl pH 8.0, 50 mM NaCl, and 10 mM DTT at 37ºC, in the absence and presence of 0.16 mg/ml or 0.08 mg/ml of αB-crystallins. The aggregation of the target proteins was monitored by measuring light scattering at 360 nm as a function of time in a V-630 spectrophotometer (JASCO) equipped with a temperature-regulated cell holder.

For the size-exclusion chromatography analyses, 8 mg/ml of ADH or 5 mg/ml of insulin was denatured in 50 mM Tris-HCl pH 8.0, 50 mM NaCl, and 30 mM EDTA or DTT at 37ºC, in the presence of 8 mg/ml of αB-crystallins. Visibly large aggregates were removed by centrifuge before the samples were applied to the column.

Results and Discussion

Circular dichroism spectral studies

The secondary structures of the wild-type and P39R mutant αB-crystallins were determined by far-UV CD spectral analysis (Figure 2A and Table 1). As expected, the mutation of Pro39 to Arg increased the α-helix content from 19.5% to 22.9%. In contrast, the β-sheet content of the P39R mutant showed a reduction to 30.2%, reduced from 35.5% in the wild-type. Few changes were observed in the β-turn and random coil contents. Because the highly conserved core domain is very stable with a dimer of β-sandwiches [10,11,12] and the C-terminal domain is thought to be highly flexible, it is likely that the changes in the secondary structure contents observed in the CD spectral analyses were due solely to structural changes at the N-terminal domain of the P39R mutant αB-crystallin. The predicted secondary structures of the N-terminal domain of wild-type αB-crystallin are composed of several helices and β-strands [15,16] (Figure 1). Therefore, it was assumed that the structural changes induced by the mutation at Pro39 to Arg are primarily limited to the N-terminal domain of αB-crystallin. It has been reported that the conformation of the N-terminal domain is related to its oligomerization states [15,16], and that the deletion of the N-terminal domain results in a larger oligomer than that of the wild-type αB-crystallin [21]. Since the Pro residue generally acts as a structural disruptor in a regular α-helix, mutation at Pro39 to Arg contributes to increase α-helix content of the N-terminal domain of αB-crystallin.

Molecular size analyses

The molecular sizes of the oligomeric complexes of wild-type and P39R mutant αB-crystallins were estimated by size exclusion chromatography and DLS analyses. Size exclusion chromatography analysis revealed slightly faster elution for the P39R

mutant (calculated as ~620 kDa) than that of the wild-type αB-crystallin (calculated as ~510 kDa, Figure 2B). These results were confirmed by the DLS data. The hydrodynamic radius of the wild-type and P39R mutant αB-crystallin was 8.0 and 8.3 nm, respectively (Table 2). These findings indicate that the conformational change at the N-terminal domain would lead to the formation of a larger assembly than that of the 24-meric wild-type αB-crystallin. This hypothesis does not contradict the assembly architecture proposed by Jehle *et al.*, in which the N-terminal domain in the 24-mer model is located around the binding area for another molecule to form even larger oligomers, such as 26 or 28-mer oligomers[16]. The conformation of the N-terminal domain of P39R mutant αB-crystallin would be preferred to form a larger assembly than that of wild-type αB-crystallin.

Chaperone-like activity

The suppression of aggregation was analyzed for denatured ADH and insulin (Figure 3). In the ADH assay, the addition of 0.8 mg/ml of wild-type or P39R mutant αB-crystallin reduced aggregation to 10.2% and 17.2% of the control, respectively, at 2000 min. Fewer αB-crystallins caused a weak suppression of aggregation; the addition of 0.16 mg/ml of wild-type or P39R mutant αB-crystallin reduced aggregation to 69.0% and 80.8% of the control level, respectively. Thus, the P39R mutant displayed a slight loss of chaperone-like activity with respect to that of the wild-type αB-crystallin.

In contrast, the P39R mutant showed a significant increase in chaperone-like activity in the insulin assay. The addition of 0.16 mg/ml of wild-type or P39R mutant αB-crystallin reduced aggregation to 10.1% and 4.0% of the control level, respectively, at 2000 min. Dilution by half of the wild-type αB-crystallin (0.08 mg/ml) resulted in

a much weaker suppression of aggregation, i.e., of 66.5% of the control, whereas dilution by half of the P39R mutant αB-crystallin retained to some extent of chaperone-like activity, i.e., of 20.7% of the control.

To elucidate how complexes are formed in chaperone-like activity assays, size exclusion chromatography was performed under conditions similar to those used for the chaperone-like activity assays. Protein concentrations were set to approximately ten times those used in the chaperone-like activity assays, in order to achieve clearer signals in the chromatograms and for subsequent PAGE analyses. For the assays of ADH and wild-type αB-crystallin, very large aggregates were eluted at the void volume, but a large portion of the αB-crystallin was eluted at 15.4 ml, just prior to the elution volume (16.0 ml) of the control of wild-type αB-crystallin (Figure 4A). The SDS-PAGE analysis of the void volume fraction demonstrated that the very large aggregates are derived from complexes of ADH and wild-type αB-crystallin, whereas the fraction at the highest peak contains primarily αB-crystallin and the fraction occurring just after the highest peak (shoulder peak at 17.0 ml) contains primarily ADH. These observations indicate that a few very large complexes (>10 MDa) of ADH and wild-type αB-crystallin are formed, but that a large portion of the αB-crystallin binds to no substrates or to only a small amount of substrate. Similar results were obtained in the assay of the ADH and P39R mutant αB-crystallin, except that the ratio of the peak of very large aggregates at the void volume to the main peak was reduced. For the assay of insulin and wild-type αB-crystallin, very large aggregates were also eluted at the void volume, but the highest peak (13.6 ml) of elution volume was observed significantly before that of the control of wild-type αB-crystallin (Figure 4B). The SDS-PAGE analysis demonstrated that both peaks are derived from complexes of insulin and

wild-type αB-crystallin. Similar results were obtained for the assay of insulin and the P39R mutant αB-crystallin, except that the ratio of the peak of very large aggregates at the void volume to the main peak was significantly increased.

The generation of the very large aggregates at the void volume corresponded to the observed chaperone-like activities. Therefore, the chaperone-like activity of αB-crystallin would depend on how the very large aggregates, the molecular size of which was estimated at more than 10 MDa, were efficiently generated. It has been previously reported that residues 57-69 and 93-107 are involved in the binding with denatured ADH[22]. Residues 57-69 are located at the end of the N-terminal domain. The conformational change at the N-terminal domain of the P39R mutant αB-crystallin would prevent residues 57-69 from interacting with denatured ADH, which would in turn suppress the formation of very large aggregates.

There is currently no information about the binding site for denatured insulin, but the mechanism of interaction clearly differs between the αB-crystallin-ADH and αB-crystallin-insulin complexes. In the insulin assay, most wild-type and P39R mutant αB-crystallins formed complexes of approximately 2,200-2,800 kDa, whereas these complexes were not observed in the ADH assay. A major difference between the conditions used for the insulin and ADH assays was the molar ratio of the substrate proteins to αB-crystallins. For the insulin assay, the molar ratios of the substrate protein to αB-crystallins were about 60 times higher than those of the ADH assay. Thus, complexes of approximately 2,200-2,800 kDa would have been responsible for the chaperone-like activity, in addition to the generation of very large aggregates at the void volume.

In conclusion, the conformational changes in the N-terminal domain of

αB-crystallin induced by the mutation of Pro39 to Arg greatly affect the oligomerization and chaperone-like activity of αB-crystallin. It has been reported that the N-terminal domain of αB-crystallin is primarily important for both its oligomerization and chaperone-like activity[21], and the hydrophobic region (residues 41-58) of the N-terminal domain is involved in the recognition of denatured proteins [23]. Our study demonstrated that the Pro39 is also a regulatory residue for the oligomerization and chaperone-like activity of αB-crystallin. The Pro-rich environment at the N-terminal domain of αB-crystallin would allow for the diversity of conformations of the N-terminal domain and is expected to be responsible for both polydisperse oligomerization and interactions with various denatured proteins.

Acknowledgements

The authors thank Prof. Y. Morimoto for his support. This work was partly supported by the System Development Program for Advanced Measurement and Analysis (Program-S) from the Japan Science and Technology Agency (JST).

References

[1] J. Horwitz, Alpha-crystallin, Exp. Eye. Res. 76 (2003) 145-153.

[2] J. Horwitz, Alpha-crystallin can function as a molecular chaperone, Proc. Natl. Acad. Sci. USA 89 (1992) 10449-10453.

[3] S.G. Bhagyalaxmi, P. Srinivas, K.A. Barton, K.R. Kumar, M. Vidyavathi, J.M. Petrash, G. Bhanuprakash Reddy, T. Padma, A novel mutation (F71L) in alphaA-crystallin with defective chaperone-like function associated with age-related cataract, Biochim. Biophys. Acta 1792 (2009) 974-981.

[4] N. Fujii, Y. Ishibashi, K. Satoh, M. Fujino, K. Harada, Simultaneous racemization and isomerization at specific aspartic acid residues in alpha B-crystallin from the aged human lens, Biochim. Biophys. Acta 1204 (1994) 157-163.

[5] N. Fujii, K. Satoh, K. Harada, Y. Ishibashi, Simultaneous stereoinversion and isomerization at specific aspartic acid residues in alpha A-crystallin from human lens, J. Biochem. 116 (1994) 663-669.

[6] P. Vicart, A. Caron, P. Guicheney, Z. Li, M.C. Prevost, A. Faure, D. Chateau, F. Chapon, F. Tome, J.M. Dupret, D. Paulin, M. Fardeau, A missense mutation in the alphaB-crystallin chaperone gene causes a desmin-related myopathy, Nat. Genet. 20 (1998) 92-95.

[7] K. Kato, Y. Inaguma, H. Ito, K. Iida, I. Iwamoto, K. Kamei, N. Ochi, H. Ohta, M. Kishikawa, Ser-59 is the major phosphorylation site in alphaB-crystallin accumulated in the brains of patients with Alexander's disease, J. Neurochem. 76 (2001) 730-736.

[8] L.E. Goldstein, J.A. Muffat, R.A. Cherny, R.D. Moir, M.H. Ericsson, X. Huang, C. Mavros, J.A. Coccia, K.Y. Faget, K.A. Fitch, C.L. Masters, R.E. Tanzi, L.T. Chylack, Jr., A.I. Bush, Cytosolic beta-amyloid deposition and supranuclear cataracts in lenses from people with Alzheimer's disease, Lancet 361 (2003) 1258-1265.

[9] R.C. Augusteyn, alpha-crystallin: a review of its structure and function, Clin. Exp. Optom. 87 (2004) 356-366.

[10] C. Bagneris, O.A. Bateman, C.E. Naylor, N. Cronin, W.C. Boelens, N.H. Keep, C.

Slingsby, Crystal structures of alpha-crystallin domain dimers of alphaB-crystallin and Hsp20, J. Mol. Biol. 392 (2009) 1242-1252.

[11] A. Laganowsky, J.L. Benesch, M. Landau, L. Ding, M.R. Sawaya, D. Cascio, Q. Huang, C.V. Robinson, J. Horwitz, D. Eisenberg, Crystal structures of truncated alphaA and alphaB crystallins reveal structural mechanisms of polydispersity important for eye lens function, Protein Sci. 19 (2010) 1031-1043.

[12] S. Jehle, P. Rajagopal, B. Bardiaux, S. Markovic, R. Kuhne, J.R. Stout, V.A. Higman, R.E. Klevit, B.J. van Rossum, H. Oschkinat, Solid-state NMR and SAXS studies provide a structural basis for the activation of alphaB-crystallin oligomers, Nat. Struct. Mol. Biol. 17 (2010) 1037-1042.

[13] J. Horwitz, Alpha crystallin: the quest for a homogeneous quaternary structure, Exp. Eye Res. 88 (2009) 190-194.

[14] A.J. Baldwin, H. Lioe, G.R. Hilton, L.A. Baker, J.L. Rubinstein, L.E. Kay, J.L. Benesch, The polydispersity of alphaB-crystallin is rationalized by an interconverting polyhedral architecture, Structure 19 (2011) 1855-1863.

[15] N. Braun, M. Zacharias, J. Peschek, A. Kastenmuller, J. Zou, M. Hanzlik, M. Haslbeck, J. Rappsilber, J. Buchner, S. Weinkauf, Multiple molecular architectures of the eye lens chaperone alphaB-crystallin elucidated by a triple hybrid approach, Proc. Natl. Acad. Sci. USA 108 (2011) 20491-20496.

[16] S. Jehle, B.S. Vollmar, B. Bardiaux, K.K. Dove, P. Rajagopal, T. Gonen, H. Oschkinat, R.E. Klevit, N-terminal domain of alphaB-crystallin provides a conformational switch for multimerization and structural heterogeneity, Proc. Natl. Acad. Sci. USA 108 (2011) 6409-6414.

[17] R.L. van Montfort, E. Basha, K.L. Friedrich, C. Slingsby, E. Vierling, Crystal structure and assembly of a eukaryotic small heat shock protein, Nat. Struct. Biol. 8 (2001) 1025-1030.

[18] K.K. Kim, R. Kim, S.H. Kim, Crystal structure of a small heat-shock protein, Nature 394 (1998) 595-599.

[19] S. Rajan, C. Horn, E.C. Abraham, Effect of oxidation of alphaA- and alphaB-crystallins on their structure, oligomerization and chaperone function, Mol. Cell Biochem. 288 (2006) 125-134.

[20] N.P. Shroff, S. Bera, M. Cherian-Shaw, E.C. Abraham, Substituted hydrophobic

and hydrophilic residues at methionine-68 influence the chaperone-like function of alphaB-crystallin, Mol. Cell Biochem. 220 (2001) 127-133.

[21] C.O. Asomugha, R. Gupta, O.P. Srivastava, Structural and functional roles of deamidation of N146 and/or truncation of NH2- or COOH-termini in human alphaB-crystallin, Mol. Vis. 17 (2011) 2407-2420.

[22] K.K. Sharma, H. Kaur, K. Kester, Functional elements in molecular chaperone alpha-crystallin: identification of binding sites in alpha B-crystallin, Biochem. Biophys. Res. Commun. 239 (1997) 217-222.

[23] J.G. Ghosh, A.K. Shenoy, Jr., J.I. Clark, N- and C-Terminal motifs in human alphaB crystallin play an important role in the recognition, selection, and solubilization of substrates, Biochemistry 45 (2006) 13847-13854.

Figure Legends

Figure 1. Amino acid sequence alignment of the N-terminal domain of αB-crystallin with wheat HSP16.9 (wHSP16.9) and MjHSP16.5. Pro residues are highlighted in boldface type. The secondary structures proposed for αB-crystallin[16] and observed in the crystal structure of wheat HSP16.9[17] are indicated at the upper and lower sides of the alignment, respectively. A gray background indicates the position of Pro39 of αB-crystallin.

Figure 2. (A) Far-UV CD spectra of wild-type and P39R mutant αB-crystallins. (B) Elution profiles of size exclusion chromatography for wild-type and P39R mutant αB-crystallins.

Figure 3. Chaperone-like activities of wild-type and P39R mutant αB-crystallins with (A) ADH (0.8 mg/ml) and (B) insulin (0.33 mg/ml) as substrate proteins at 37ºC.

Figure 4. Elution profiles and SDS-PAGE analyses of fractions of size exclusion chromatography for the complexes of (A) denatured ADH and (B) denatured insulin with wild-type and P39R mutant αB-crystallins. The elution profiles of the control of wild-type and P39R mutant αB-crystallins are overlaid. SDS-PAGE for the fraction of the void volume concentrated tenfold for the insulin and wild-type αB-crystallin assay is shown in the inset of elution profiles.

Tables for

A P39R mutation at the N-terminal domain of human αB-crystallin regulates its oligomeric state and chaperone-like activity

Nobutaka Numoto, Akiko Kita, Noriko Fujii, Kunio Miki

Table 1. Secondary structure contents (%) of wild-type and P39R mutant αB-crystallins.

	α helix	β sheet	β turn	Random coil
Wild-type αB	19.5	35.5	18.8	26.2
P39R	22.9	30.2	19.6	27.2

Table 2. Hydrodynamic radius of wild-type and P39R mutant αB-crystallins.

	Rh (nm)	Cp/Rh (%)
Wild-type αB	8.0	14.5
P39R	8.3	18.3

Rh, hydrodynamic radius

Cp/Rh, polydispersity index

Figure 1

Click here to download high resolution image

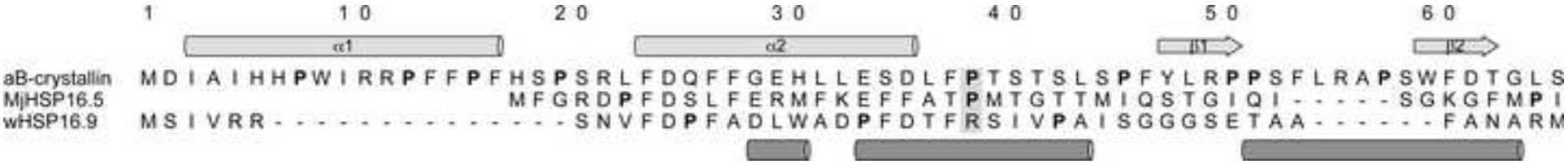

Figure 2

Click here to download high resolution image

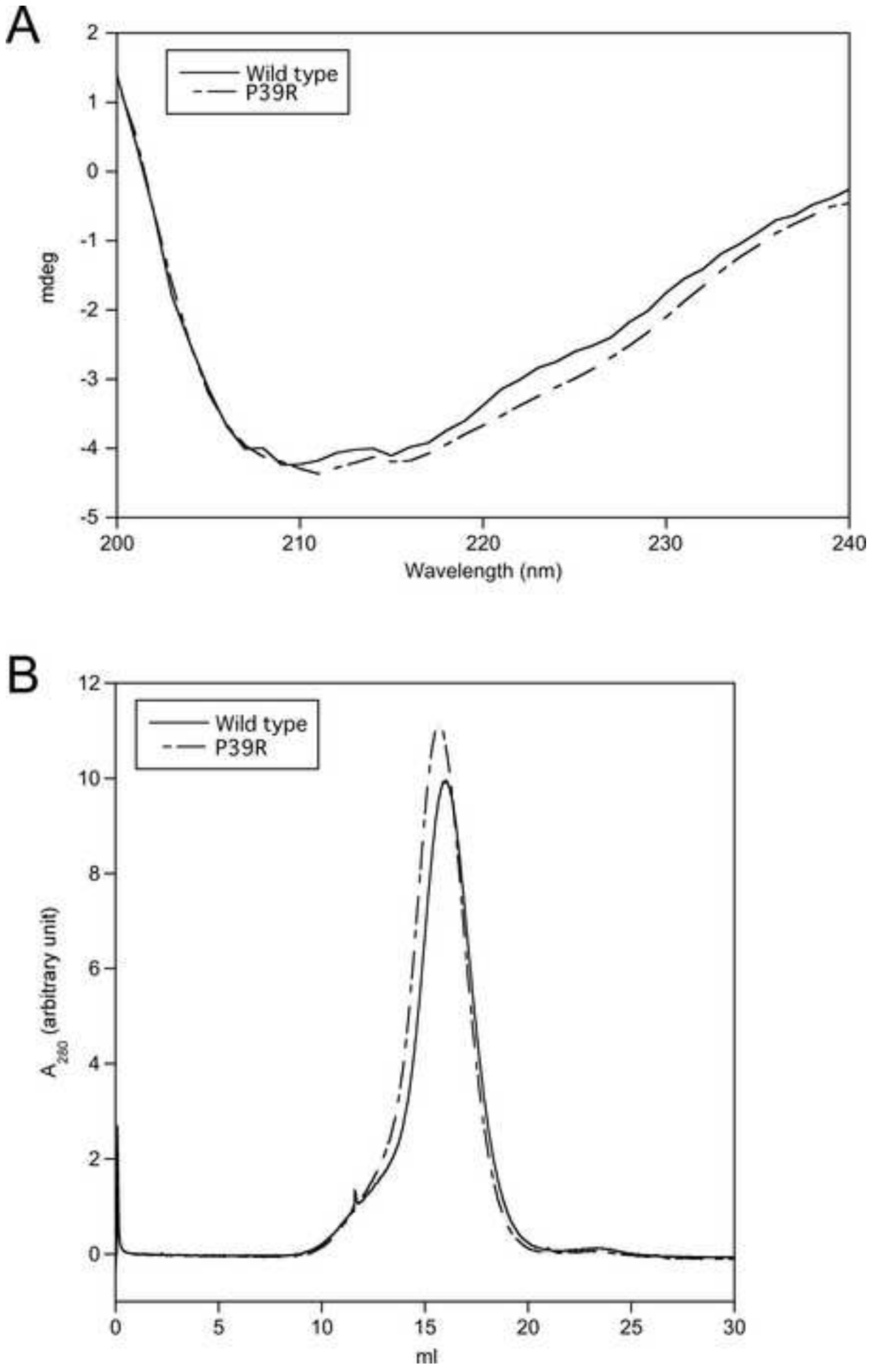

Figure 3

Click here to download high resolution image

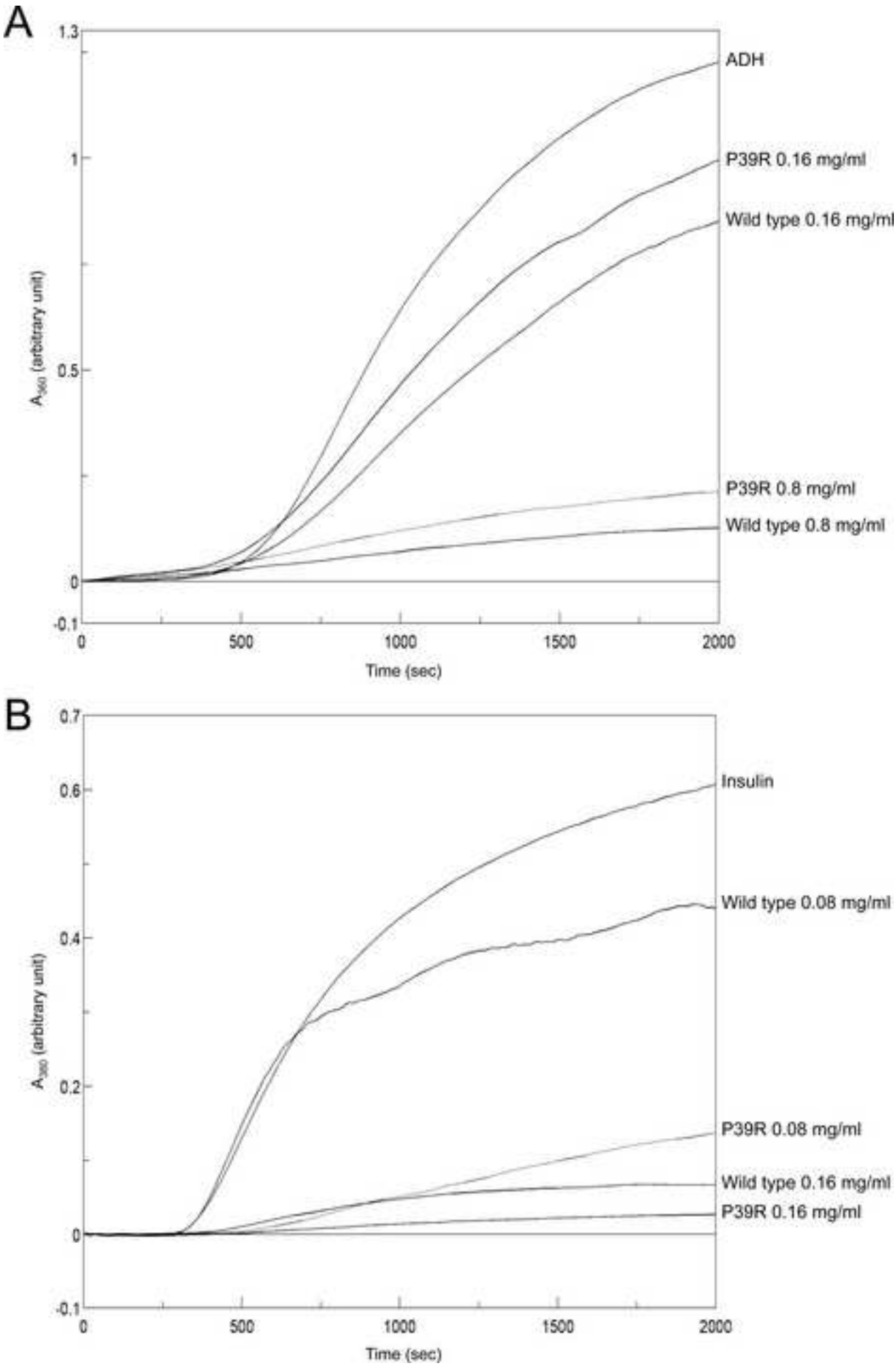

Figure 4

Click here to download high resolution image